PHYSICAL REVIEW B **86**, 100504(R) (2012)

Topological indices, defects, and Majorana fermions in chiral superconductors

Daichi Asahi[1] and Naoto Nagaosa[1,2]

[1]*Department of Applied Physics, University of Tokyo, Tokyo 113-8656, Japan*

[2]*Cross Correlated Materials Research Group (CMRG) and Correlated Electron Research Group (CERG), ASI, RIKEN, Wako 351-0198, Japan*

(Received 29 March 2012; revised manuscript received 29 August 2012; published 14 September 2012)

We study theoretically the role of topological invariants to protect the Majorana fermions in a model of two-dimensional (2D) chiral superconductors which belong to class D of the topological periodic table. A rich phase diagram is revealed. Each phase is characterized by the topological invariants for 2D (Z) and 1D (Z_2), which lead to the Majorana fermion at the edge dislocation and the core of the vortex. Interference of the Majorana fermions originating from the different topological invariants is studied. The stability of the Majorana fermion with respect to the interlayer coupling, i.e., in 3D, is also examined.

DOI: 10.1103/PhysRevB.86.100504 PACS number(s): 74.20.−z, 71.10.Pm, 74.62.Dh

Topological classification of the electronic states in solids has shed light on the band structure of solids and also the superconductivity.[1] Initiated by the proposal of the Z_2 topological invariant and the quantum spin Hall effect in a two-dimensional (2D) spin-orbit coupled system[2] and its extension to three dimensions (3D),[3] the more generic topological classification scheme, i.e., the topological periodic table, is now available based on three symmetries, i.e., time-reversal (Θ), particle-hole (Ξ), and chiral (Π) symmetries.[4,5] Here Ξ symmetry is due to the superconductivity in the usual situation. There are ten classes, and the topological invariant is specified depending on the dimensionality d of the system to characterize the nontrivial topological states. Later, this "tenfold way" has been extended to classification including textures such as domain walls and dislocations.[6] In this case, the dimensionality D of the real space manifold surrounding the texture plays a key role, and $\delta = d - D$ replaces d for the topological classification.[6] In the topological periodic table, one can recognize the periodicity called the Bott periodicity, which relates the different classes in the "diagonal" direction. This periodicity can be understood by the continuous mapping of the Hamiltonian connecting the different classes and different δ by one. On the other hand, one can also consider the connection in the "horizontal" direction, i.e., dimensional reduction.[7] As an example, class AII has been characterized by Z_2 both for $\delta = 3$ and $\delta = 2$. The former corresponds to the Z_2 invariant corresponding to a strong topological insulator (TI) in 3D, while the latter corresponds to the quantum spin Hall system in a 2D ($D = 0$) or a weak TI in 3D ($D = 1$). Namely, a 3D system is characterized by four Z_2 topological invariants $\nu_0;\nu_1\nu_2\nu_3$, where $\nu_0 = 1$ indicates a strong TI, while $\nu_0 = 0$ with at least one nonzero $\nu_{1,2,3}$ means a weak TI. These $\nu_{1,2,3}$ are the topological invariants for $\delta = 3 - 1 = 2$, and guarantee the existence of a gapless one-dimensional mode along the dislocation.[8] A recent study has shown that dislocations can host Kramers pairs of zero modes in 2D TIs.[9]

This topological periodic table provides a powerful guiding principle also for topological superconductors (TSs). Especially, the Majorana fermions expected to appear at the edge or the core of the vortex in TSs attract intensive interests from the viewpoint of quantum information technology.[10–15] Therefore, it is an important theoretical issue to design the Majorana fermions in realistic systems. Proximity-induced superconductivity in 3D TIs,[16–21] the superconductivity in a doped TI $Cu_xBi_2Se_3$,[22–26] the possible TSs in noncentrosymmetric systems with Rashba spin splitting,[27–37] and p-wave superconductivity in Sr_2RuO_4 (Refs. 38 and 39) are promising candidates as hosts of the Majorana fermions. Recently, signatures of Majorana fermions have been observed by electrical measurements on InSb nanowires contacted with a superconducting electrode.[40] As pointed out in Ref. 41, most of the theoretical proposals for the Majorana fermions are based on two models, i.e., p-wave pairing in the one-dimensional spinless fermions (Kitaev model[10]) and the $p + ip$ pairing superconductor.

In this Rapid Communication, we study theoretically the topological invariants and their relation to the protected Majorana bound states in a model of class D chiral superconductors containing both the Kitaev model and a $p + ip$ superconductor in the limiting cases. The topological invariant for class D is 0 for $\delta = 3$, Z for $\delta = 2$, and Z_2 for $\delta = 1$. Therefore, there is no "strong TS" in 3D, while the 2D system is characterized by a Z topological invariant and the one-dimensional (1D) system by a Z_2 topological invariant. The purpose of the present Rapid Communication is to reveal the topological phase diagram characterized by these invariants, and the associated Majorana fermions at textures such as dislocations and vortices.

We consider a generalized model of the $p + ip$ wave superconductor on a square lattice in 2D. The Hamiltonian can be written as $H = \sum_{\boldsymbol{k}} C_{\boldsymbol{k}}^\dagger H(\boldsymbol{k}) C_{\boldsymbol{k}}$, with

$$H(\boldsymbol{k}) = \begin{pmatrix} 2t_x \cos k_x + 2t_y \cos k_y - \mu & d_x \sin k_x - i d_y \sin k_y \\ d_x \sin k_x + i d_y \sin k_y & \mu - 2t_x \cos k_x - 2t_y \cos k_y \end{pmatrix}, \tag{1}$$

and $C_{\mathbf{k}}^\dagger = (c_{\mathbf{k}}^\dagger, c_{-\mathbf{k}})$. This 2×2 Hamiltonian matrix can be expressed as $H(\boldsymbol{k}) = H(k_x,k_y) = \boldsymbol{h}(\boldsymbol{k}) \cdot \boldsymbol{\sigma}$, where $\boldsymbol{\sigma} = (\sigma^x,\sigma^y,\sigma^z)$ is the vector of Pauli matrices. Since $(C_{-\mathbf{k}}^\dagger)^T = \sigma^x C_{\mathbf{k}}$, $H(\mathbf{k})$ should satisfy

$$H(\boldsymbol{k}) = -\sigma^x H(-\boldsymbol{k})^T \sigma^x, \tag{2}$$

where T means the transpose. This condition leads to the relation[41]

$$h_{x,y}(\boldsymbol{k}) = -h_{x,y}(-\boldsymbol{k}), \quad h_z(\boldsymbol{k}) = h_z(-\boldsymbol{k}). \tag{3}$$

Therefore, for time-reversal invariant momenta (TRIM), which satisfy $\boldsymbol{k} \equiv -\boldsymbol{k}$, only $h_z(\boldsymbol{k})$ cannot be nonzero, i.e., $\boldsymbol{h}(\boldsymbol{k})$ points either in the $+z$ or $-z$ directions as long as the gap opens, i.e., $|\boldsymbol{h}(\boldsymbol{k})| > 0$. There are four TRIM in this 2D model, i.e., $\boldsymbol{k}_\alpha = (0,0),(\pi,0),(0,\pi)$, and (π,π), and the sign $s_\alpha = \pm 1$ of the corresponding h_z. As will be discussed, s_α determines the Z_2 topological invariants and the parity of the Z invariant.

Now let us start with the Z_2 invariant. For this purpose, let us consider the 1D Hamiltonian with fixed $k_x = \pi$ in Eq. (1), i.e.,

$$H(k_x = \pi, k_y) = \begin{pmatrix} -2t_x + 2t_y \cos(k_y) - \mu & -id_y \sin(k_y) \\ id_y \sin(k_y) & \mu + 2t_x - 2t_y \cos(k_y) \end{pmatrix}, \tag{4}$$

which is nothing but the Kitaev model for a one-dimensional topological superconductor.[10] The Z_2 topological invariant ν_x is related to the "polarization"[7]

$$\frac{\nu_x}{2} = P(k_x) = \int_{-\pi}^{\pi} \frac{dk_y}{2\pi} a_y(k_x,k_y) \bmod 1 \tag{5}$$

given by the Berry phase vector potential $a_j(k_x,k_y) = (-i)\sum_{n:\text{occupied}} \langle n\boldsymbol{k}|\partial/\partial \boldsymbol{k}_j|n\boldsymbol{k}\rangle$, and is given by $(-1)^{\nu_x} = s_{(\pi,0)}s_{(\pi,\pi)}$.[41–44] Therefore, we can easily obtain the Z_2 topological invariant ν_x as

$$\nu_x = \begin{cases} 1 & \text{for} \quad |t_x + \frac{\mu}{2}| < |t_y|, \\ 0 & \text{for} \quad |t_x + \frac{\mu}{2}| > |t_y|. \end{cases} \tag{6}$$

The topological invariant ν_x' for $k_x = 0$ can be calculated also in a similar way. From these equations, it is clear that the strengths of d_x and d_y are not related to the topological numbers if they have finite values. The Z_2 invariants ν_y, ν_y' are obtained in a similar way.

On the other hand, the Z topological invariant ν is nothing but the Chern number, i.e., the wrapping number of the mapping from the first Brillouin zone (BZ) of $\boldsymbol{k}$ to the unit sphere $\boldsymbol{h}(\boldsymbol{k})/|\boldsymbol{h}(\boldsymbol{k})|$ and is given by

$$\nu = \iint_{\text{BZ}} \frac{dk_x dk_y}{2\pi} \{\partial_{k_x} a_y(k_x,k_y) - \partial_{k_y} a_x(k_x,k_y)\}. \tag{7}$$

Equations (5) and (7) lead to the relation[7,30,41–44]

$$\nu_x + \nu_x' = \nu_y + \nu_y' = \nu \bmod 2. \tag{8}$$

In summary, our model is characterized by the Z topological invariant ν and two Z_2 topological invariants ν_x and ν_y. This is the general result, and superconductors in class D in 2D are characterized by $\nu : \nu_x\nu_y$. From the above consideration, these topological invariants depend on the hopping integrals t_x, t_y and the chemical potential μ, while they do not depend on the pairing amplitudes d_x, d_y as long as they are finite. Therefore, we show in Fig. 1 the phase diagram of the present model in the plane of (t_x,t_y) for fixed μ. The lines where the energy gap closes divide the (t_x,t_y) plane into nine domains. Electronic states are characterized by topological invariants in each domain. When $\frac{|\mu|}{2}$ is larger than $|t_x| + |t_y|$, i.e., domain V, the pairing state is topologically trivial since it corresponds to the strong coupling limit. In domains II, III, VII, and VIII, electronic states have both Z and Z_2 topological invariants.

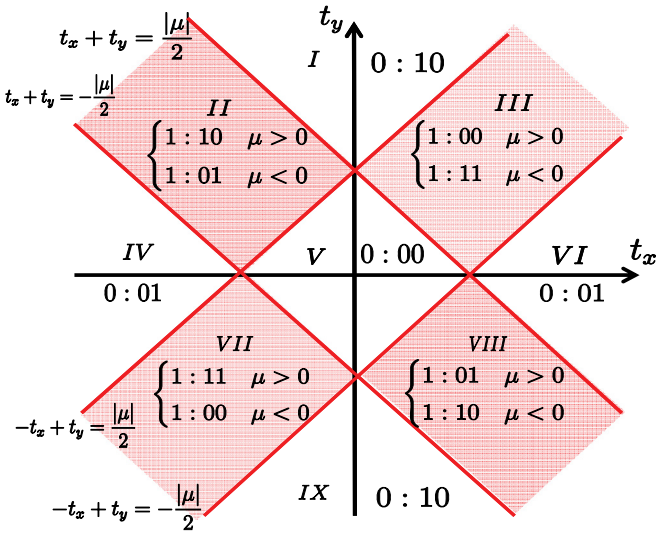

FIG. 1. (Color online) The topological phase diagram of a model in Eq. (1) for chiral superconductors in 2D characterized by $\nu : \nu_x\nu_y$. The lines where the energy gap closes divide the (t_x,t_y) plane into nine domains. The system is a strong topological superconductor ($\nu = 1$) in domains II, III, VII, and IX, with $\nu = 0$ but some of Z_2 invariants being nonzero. In domain V, the system is the trivial strong coupling superconductor.

Note that the sign of the chemical potential μ matters for the Z_2 invariants. In domains I, IV, VI, and IX, the anisotropy between t_x and t_y is large and hence the system behaves basically as the weakly coupled chains of 1D Kitaev models, and the system has only 1D Z_2 topological invariants but Z topological invariant $\nu = 0$, so they are weak topological states.

Now we turn to the consequences of the topological invariants. The Z_2 invariant ν_x (ν_y) ensures that the propagating Majorana fermion channels appear at the edge along the x direction (y direction). They have zero-energy states at $k_x = \pi$ ($k_y = \pi$). Also the edge dislocation offers the stage for the zero-energy Majorana bound state when the following equation is satisfied (see Fig. 2):

$$\mathbf{B} \cdot \mathbf{G} = 1 \bmod 2. \tag{9}$$

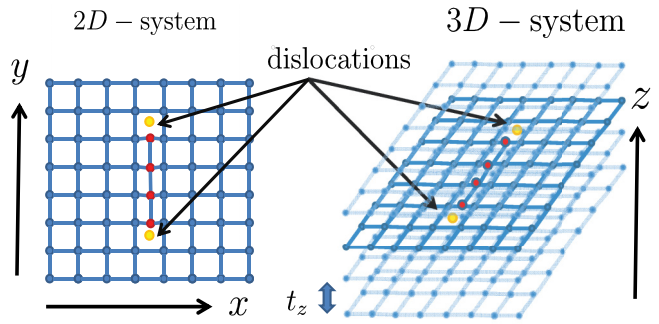

FIG. 2. (Color online) The edge dislocations (indicated by yellow points) in two- and three-dimensional systems. The 3D system is made by stacking 2D systems and adding a hopping integral along the z direction with the edge dislocation isolated on a layer.

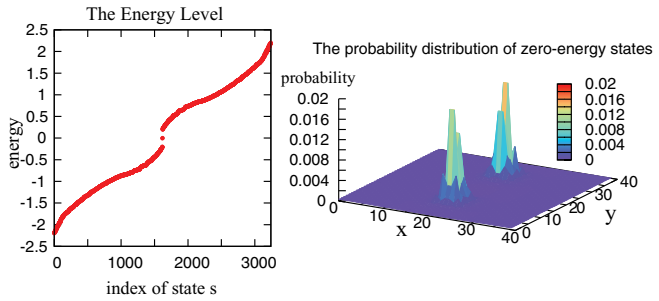

FIG. 3. (Color online) The energy levels and the probability distribution of zero-energy states at each site in the presence of edge dislocations: The left panel indicates the energy levels. The right panel indicates the probability distribution for the zero-energy states. The zero-energy Majorana bound states appear at each of the edge dislocations.

In this equation, we define $\mathbf{G} = \frac{1}{2\pi}(\nu_x \mathbf{b}_x + \nu_y \mathbf{b}_y)$. $\mathbf{b}_x$ and $\mathbf{b}_y$ are the reciprocal lattice vectors of the x and y directions, respectively, and $\mathbf{B}$ is the Burgers vector characterizing the dislocation. We numerically calculate these zero-energy states as follows. To introduce a periodic boundary condition, we introduce two edge dislocations with the Burgers vector $\mathbf{B} = \pm\mathbf{e}_x$. We represent two edge dislocations by adding lattice sites between them. Edge dislocations are separated by a half system size. Calculations were done on a 40×40 unit cell system with a periodic boundary condition along the x and y directions. The parameters are $t_x = 0.5$, $t_y = 0.5$, $d_x = 0.6$, $d_y = 0.6$, and $\mu = -0.2$. In these parameters, the topological invariants are 1 : 11. In this case, $\mathbf{G} = \frac{1}{2\pi}(\mathbf{b}_x + \mathbf{b}_y)$ and $\mathbf{B} = \pm\mathbf{e}_x$, $\mathbf{B} \cdot \mathbf{G} = 1$ is satisfied, so zero-energy states appear at the edge dislocations.

The results of our numerical calculations are shown in Fig. 3. The left panel of Fig. 3 indicates the energy levels of our model in the presence of edge dislocations. It is clear that zero-energy states exist, which are twofold degenerate because the two edge dislocations are present in the system. The right panel of Fig. 3 indicates the probability distribution of the zero-energy states. Zero-energy states are localized at each edge dislocation.

In the presence of edge dislocations with the Burgers vector $\mathbf{B} = \pm\mathbf{e}_x$, zero-energy states appear in domains I, II, VII, and IX in Fig. 1 in the case of $\mu > 0$ and zero-energy states appear in domains I, III, VIII, and IX in Fig. 1 in the case of $\mu < 0$. In particular, zero-energy states in domains I and IX can be intuitively interpreted as follows. The weak topological superconductors in these domains are adiabatically connected to a stack of the Kitaev models[10] for a 1D topological superconductor along the y direction. In the presence of edge dislocations, the edges of the 1D topological superconductor appear at edge dislocations as shown in Fig. 2, so zero-energy states appear there. In general, the existence of zero-energy states is proved by the same method as in Ref. 8.

Next we consider the interference of the Z and Z_2 topological invariants, which is realized in the present model. When Z is nonzero, the zero-energy Majorana bound state is realized at the core of the vortex.[13,14] It is expected that, if the dislocations are in the crystal, they act as the pinning centers of the vortex, and hence there are two reasons for the existence of the Majorana bound states when the Z_2 invariant is 1. This situation occurs in domains II, III, VII, and VIII in Fig. 1, and the interference of these two mechanisms is an issue. Figure 4 summarizes the calculated results, in which there are dislocations and vortex cores at same positions. The probability distributions are plotted for the zero-energy states, if any.

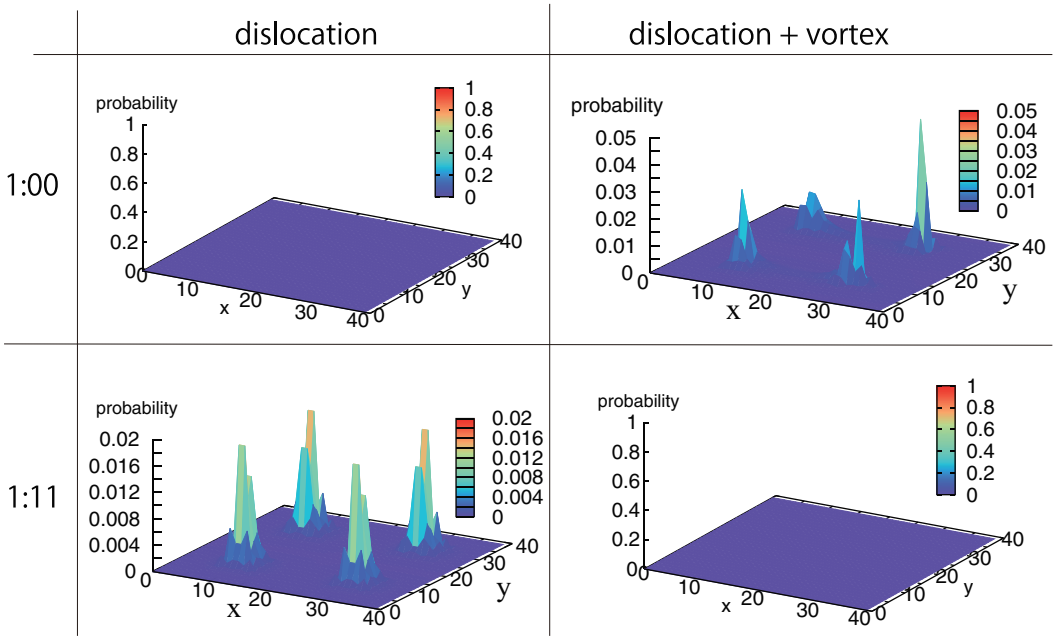

FIG. 4. (Color online) The interaction between zero-energy states localized at edge dislocations and zero-energy states localized at vortex cores: This figure shows the probability distribution of zero-energy states at each lattice site in each case. The interaction between zero-energy states at edge dislocations and zero-energy states at vortex cores eliminates zero-energy states when dislocations and vortex cores exist at the same positions.

To introduce a periodic boundary condition, we introduce two vortices with the winding number 1 and two vortices with the winding number -1. We consider the two cases of topological invariants $1:00$ (upper panels) and $1:11$ (lower panels). The parameters are $t_x = 0.5$, $t_y = 0.5$, $d_x = 0.6$, $d_y = 0.6$, $\mu = 0.2$ for the former, while they are $t_x = 0.5$, $t_y = 0.5$, $d_x = 0.6$, $d_y = 0.6$, $\mu = -0.2$ for the latter. Calculations were done on a 40×40 unit cell system with a periodic boundary condition along the x and y directions. There are dislocations and vortex cores at the same positions in the right panels while only dislocations are there in the left panels. They are separated from each other by a half system size. In the case of the topological invariants $1:00$, zero-energy states do not appear at the edge dislocations. Zero-energy states appear when the dislocations and vortices exist at the same time because of the Z invariant $\nu = 1$ and vortices. We have also confirmed that the zero-energy states appear with only the vortices. In the case of the topological invariants $1:11$, zero-energy states appear when dislocations exist but vortices do not exist. The interaction between zero-energy states at edge dislocations and at vortex cores eliminates the zero-energy states when they coexist at the same position. This can be naturally understood that the two Majorana bound states due to the Z and Z_2 invariants interact with each other as they approach each other, and lift the degeneracy to have finite energies.

We generalize this model into a model in 3D. The 3D model is constructed as a stack of 2D models with a hopping integral t_z along the z direction as shown in Fig. 2. t_z causes the finite region where the energy gap closes in the (t_x,t_y) plane. The energy gap closes in the domain, which satisfies $|t_x + t_y - \frac{\mu}{2}| < |t_z|$, $|-t_x + t_y - \frac{\mu}{2}| < |t_z|$, $|t_x - t_y - \frac{\mu}{2}| < |t_z|$, or $|-t_x - t_y - \frac{\mu}{2}| < |t_z|$. The domain where the energy gap opens is connected to the domain of $t_z = 0$, so electronic states in the domain have the same topological invariants as the 2D model, while the topology is trivial for class D in 3D. We introduce a similar defect as a 2D system, as indicated in Fig. 2. These defects are not edge dislocations. One layer has the same defect as the 2D system and the other layers do not have it. We ensure that zero-energy states appear at those defects in the same manner as the 2D system by numerical calculations. The parameters are $t_x = 0.5$, $t_y = 0.5$, $t_z = 0.1$, $d_x = 0.6$, $d_y = 0.6$, and $\mu = -0.5$. In this case, the electronic state is adiabatically connected to the state in domain III in the case of $\mu < 0$ in Fig. 1. If $t_z = 0$, zero-energy states appear in these parameters because the state in domain III in the case of $\mu < 0$ in Fig. 1 has topological invariants $1:11$ and one layer has edge dislocations with the Burgers vector $\mathbf{B} = \pm\mathbf{e}_x$. Calculations were done on a $10 \times 20 \times 10$ unit cell system with a periodic boundary condition along the x, y, and z directions. We found that these zero-energy states survive a finite-value z direction hopping integral t_z unless the energy gap closes. This edge dislocation is a zero-dimensional (0D) object, and we need a $D = 2$ sphere to enclose this defect in 3D, and hence $\delta = 3 - 2 = 1$. Therefore, the Z_2 invariant protects the existence of the Majorana zero-energy bound state. This is an example of the "weak-weak" topological superconductor, where the topological invariant reduced by two dimensions is relevant. This indicates that Majorana fermions can exist even in a 3D system.

Now we discuss the relevance of the present results to the real materials. There are several candidates for the chiral superconductors. The 2D Rashba system in a semiconductor with proximity to the s-wave superconductor and the ferromagnet is a promising candidate, which shows spinless $p + ip$ pairing.[28,29,31,32] The electron density is considered to be small and concentrated near the Γ point of the first Brillouin zone. Therefore, usually the continuum approximation is used to describe this system. In our phase diagram (Fig. 1), this situation corresponds to domain VII with $t_x = t_y < 0$ with a negative chemical potential, which is characterized by $\nu = 1$ and $\nu_x = \nu_y = 0$. Therefore, we do expect the Majorana bound state at the core of the vortex, while there is no Majorana bound state at the edge dislocation. To realize a more interesting situation where both ν and $\nu_{x,y}$ are nonzero, it is required to have the Fermi pocket near TRIM other than the Γ point. This is the case for semiconductors such as PbTe and SnTe which have the Fermi pocket at the L point in the fcc Brillouin zone.[45] So, quantum wells made by these materials have the Fermi pocket at the (π,π) point. 3C-SiC and 6H-SiC have the Fermi pocket at the M point in hexagonal BZ. The thin film can be used to realize the situation where both ν and $\nu_{x,y}$ are nonzero.

Another interesting candidate is Sr_2RuO_4,[38,39] which is a layered material and believed to be a quasi-2D $p + ip$ superconductor with a nonzero Z invariant. In this system, there remains the spin degeneracy of the Fermi surface, and hence the Hamiltonian matrix is at least 4×4 instead of the 2×2 discussed in this Rapid Communication. This means that the Z_2 invariants are zero due to this degeneracy, although the Z invariant can be nonzero. However, a detailed analysis taking into account the three bands, i.e., α, β, and γ bands,[46,47] has revealed that the edge dislocations can host two Majorana fermions at each layer.[48] Unpaired Majorana fermions can appear at the two ends of the edge dislocations, if a nonzero supercurrent is maintained along the edge dislocation, as in the case of vortex lines.[49]

To summarize, we have studied a model of chiral superconductors including both the Kitaev model in 1D and $p + ip$ superconductor in 2D as limiting cases. This model shows a rich phase diagram (Fig. 1) characterized by the Z and Z_2 topological invariants, which control the appearance of Majorana bound states at the edge dislocations and vortex cores. This offers an explicit case where the topological periodic table can be successfully applied, including the topological textures, and the presence of the Majorana bound states are shown also numerically.

The authors acknowledge fruitful discussions with Yukio Tanaka and Sho Nakosai. This work is supported by Grants-in-Aid for Scientific Research (Grants No. 17071007, No. 17071005, No. 19048008, No. 19048015, No. 22103005, No. 22340096, and No. 21244053) from the Ministry of Education, Culture, Sports, Science and Technology of Japan, Strategic International Cooperative Program (Joint Research Type) from Japan Science and Technology Agency, and Funding Program for World-Leading Innovative RD on Science and Technology (FIRST Program).

[1]For recent review articles, see M. Z. Hasan and C. L. Kane, Rev. Mod. Phys. **82**, 3045 (2010); X.-L. Qi and S.-C. Zhang, *ibid*. **83**, 1057 (2011).
[2]C. L. Kane and E. J. Mele, Phys. Rev. Lett. **95**, 226801 (2005).
[3]J. E. Moore and L. Balents, Phys. Rev. B **75**, 121306 (2007); L. Fu and C. L. Kane, *ibid*. **76**, 045302 (2007); R. Roy, *ibid*. **79**, 195321 (2009).
[4]A. P. Schnyder, S. Ryu, A. Furusaki, and A. W. W. Ludwig, Phys. Rev. B **78**, 195125 (2008).
[5]A. Kitaev, in *Advances in Theoretical Physics: Landau Memorial Conference*, edited by V. Lebedev and M. Feigel'man, AIP Conf. Proc., Vol. 1134 (AIP, Melville, NY, 2009), p. 22.
[6]J. C. Y. Teo and C. L. Kane, Phys. Rev. B **82**, 115120 (2010).
[7]X.-L. Qi, T. L. Hughes, and S.-C. Zhang, Phys. Rev. B **78**, 195424 (2008).
[8]Y. Ran, Y. Zhang, and A. Vishwanath, Nat. Phys. **5**, 298 (2009).
[9]V. Juricic, A. Mesaros, R. J. Slager, and J. Zaanen, Phys. Rev. Lett. **108**, 106403 (2012).
[10]A. Y. Kitaev, Phys. Usp. **44**, 131 (2001).
[11]C. Nayak, S. H. Simon, A. Stern, M. Freedman, and S. Das Sarma, Rev. Mod. Phys. **80**, 1083 (2008).
[12]S. Das Sarma, C. Nayak, and S. Tewari, Phys. Rev. B **73**, 220502 (2006).
[13]N. Read and D. Green, Phys. Rev. B **61**, 10267 (2000).
[14]D. A. Ivanov, Phys. Rev. Lett. **86**, 268 (2001).
[15]Y. Tanaka, M. Sato, and N. Nagaosa, J. Phys. Soc. Jpn. **81**, 011013 (2012).
[16]L. Fu and C. L. Kane, Phys. Rev. Lett. **100**, 096407 (2008).
[17]L. Fu and C. L. Kane, Phys. Rev. Lett. **102**, 216403 (2009).
[18]A. R. Akhmerov, J. Nilsson, and C. W. J. Beenakker, Phys. Rev. Lett. **102**, 216404 (2009).
[19]K. T. Law, P. A. Lee, and T. K. Ng, Phys. Rev. Lett. **103**, 237001 (2009).
[20]Y. Tanaka, T. Yokoyama, and N. Nagaosa, Phys. Rev. Lett. **103**, 107002 (2009).
[21]J. Linder, Y. Tanaka, T. Yokoyama, A. Sudbo, and N. Nagaosa, Phys. Rev. Lett. **104**, 067001 (2010).
[22]Y. S. Hor, A. J. Williams, J. G. Checkelsky, P. Roushan, J. Seo, Q. Xu, H. W. Zandbergen, A. Yazdani, N. P. Ong, and R. J. Cava, Phys. Rev. Lett. **104**, 057001 (2010).
[23]L. Fu and E. Berg, Phys. Rev. Lett. **105**, 097001 (2010).
[24]S. Sasaki, M. Kriener, K. Segawa, K. Yada, Y. Tanaka, M. Sato, and Y. Ando, Phys. Rev. Lett. **107**, 217001 (2011).
[25]A. Yamakage, K. Yada, M. Sato, and Y. Tanaka, Phys. Rev. B **85**, 180509(R) (2012).
[26]T. H. Hsieh and L. Fu, Phys. Rev. Lett. **108**, 107005 (2012).
[27]Y. Tanaka, T. Yokoyama, A. V. Balatsky, and N. Nagaosa, Phys. Rev. B **79**, 060505 (2009).
[28]M. Sato and S. Fujimoto, Phys. Rev. B **79**, 094504 (2009).
[29]J. D. Sau, R. M. Lutchyn, S. Tewari, and S. Das Sarma, Phys. Rev. Lett. **104**, 040502 (2010).
[30]X.-L. Qi, T. L. Hughes, and S.-C. Zhang, Phys. Rev. B **82**, 184516 (2010).
[31]R. M. Lutchyn, J. D. Sau, and S. Das Sarma, Phys. Rev. Lett. **105**, 077001 (2010).
[32]J. Alicea, Phys. Rev. B **81**, 125318 (2010).
[33]Y. Oreg, G. Refael, and F. von Oppen, Phys. Rev. Lett. **105**, 177002 (2010).
[34]A. Cook and M. Franz, Phys. Rev. B **84**, 201105 (2011).
[35]M. Sato, Y. Takahashi, and S. Fujimoto, Phys. Rev. Lett. **103**, 020401 (2009).
[36]Y. Tanaka, Y. Mizuno, T. Yokoyama, K. Yada, and M. Sato, Phys. Rev. Lett. **105**, 097002 (2010).
[37]K. Yada, M. Sato, Y. Tanaka, and T. Yokoyama, Phys. Rev. B **83**, 064505 (2011).
[38]A. P. MacKenzie and Y. Maeno, Rev. Mod. Phys. **75**, 657 (2003).
[39]S. Kashiwaya, H. Kashiwaya, H. Kambara, T. Furuta, H. Yaguchi, Y. Tanaka, and Y. Maeno, Phys. Rev. Lett. **107**, 077003 (2011)
[40]V. Mourik *et al*., Science **336**, 1003 (2012).
[41]J. Alicea, Rep. Prog. Phys. **75**, 076501 (2012).
[42]A. M. Turner *et al*., Phys. Rev. B **85**, 165120 (2012).
[43]M. Sato, Phys. Rev. B **79**, 214526 (2009).
[44]M. Sato, Phys. Rev. B **81**, 220504(R) (2010).
[45]T. H. Hsieh, H. Lin, J. Liu, W. Duan, A. Bansil, and L. Fu, Nat. Commun. **3**, 982 (2012).
[46]D. F. Agterberg, T. M. Rice, and M. Sigrist, Phys. Rev. Lett. **78**, 3374 (1997).
[47]S. Raghu, A. Kapitulnik, and S. A. Kivelson, Phys. Rev. Lett. **105**, 136401 (2010).
[48]D. Asahi and N. Nagaosa (unpublished).
[49]B. Seradjeh and E. Grosfeld, Phys. Rev. B **83**, 174521 (2011).